GENETICS, 2025, 229(3), iyaf005
https://doi.org/10.1093/genetics/iyaf005
Advance Access Publication Date: 10 January 2025
Investigation

Functions of the Bloom syndrome helicase N-terminal intrinsically disordered region

Colleen C. Bereda [1,†] Evan B. Dewey [2,3,4,†] Mohamed A. Nasr,[5] Venkat R. Chirasani [6] Jeff Sekelsky [1,2,3,5,*]

[1]Department of Biology, University of North Carolina at Chapel Hill, Chapel Hill, NC 27599, USA
[2]Lineberger Comprehensive Cancer Center, University of North Carolina at Chapel Hill, Chapel Hill, NC 27599, USA
[3]Integrative Program for Biological and Genome Sciences, University of North Carolina at Chapel Hill, Chapel Hill, NC 27599, USA
[4]Department of Biology, Winthrop University, Rock Hill, SC 29733, USA
[5]Curriculum in Genetics and Molecular Biology, University of North Carolina at Chapel Hill, Chapel Hill, NC 27599, USA
[6]R.L. Juliano Structural Bioinformatics Core, University of North Carolina at Chapel Hill, Chapel Hill, NC 27599, USA

*Corresponding author: Department of Biology, University of North Carolina at Chapel Hill, Chapel Hill, NC 27599, USA. Email: sekelsky@unc.edu
[†]These authors contributed equally.

Bloom syndrome helicase (Blm) is a RecQ family helicase involved in DNA repair, cell cycle progression, and development. Pathogenic variants in human *BLM* cause the autosomal recessive disorder Bloom Syndrome, characterized by predisposition to numerous types of cancer. Prior studies of *Drosophila Blm* mutants lacking helicase activity or protein have shown sensitivity to DNA damaging agents, defects in repairing DNA double-strand breaks (DSBs), female sterility, and improper segregation of chromosomes in meiosis. Blm orthologs have a well-conserved and highly structured RecQ helicase domain, but more than half of the protein, particularly in the N-terminus, is predicted to be intrinsically disordered. Because this region is poorly conserved across metazoa, we compared closely related species to identify regions of conservation that might be associated with important functions. We deleted 2 *Drosophila*-conserved regions in *Drosophila melanogaster* using CRISPR/Cas9 gene editing and assessed the effects on several Blm functions. Each deletion had distinct effects. Deletion of either conserved region 1 (CR1) or CR2 compromised DSB repair through synthesis-dependent strand annealing and resulted in increased mitotic crossovers. In contrast, CR2 is critical for embryonic development, but CR1 is less important. Loss of CR1 leads to defects in meiotic crossover designation and patterning but does not impact meiotic chromosome segregation, whereas deletion of CR2 does not result in significant meiotic defects. Thus, while the 2 regions have overlapping functions, there are distinct roles facilitated by each. These results provide novel insights into functions of the N-terminal region of Blm helicase.

Keywords: Bloom syndrome helicase; recombination; DNA repair; intrinsically disordered region

Introduction

Bloom syndrome helicase (Blm in *Drosophila*; BLM in humans) is an ATP-dependent, RecQ family helicase (Ellis *et al.* 1995; Adams *et al.* 2003; Larsen and Hickson 2013). Blm is conserved across protists, plants, fungi, and animals, with roles in homology-directed DNA repair (HDR), cell cycle progression, meiosis, and development (Dutertre *et al.* 2000; Imamura *et al.* 2001; Wu and Hickson 2003; McVey *et al.* 2007; Wu 2007; Lafave *et al.* 2014; Hatkevich *et al.* 2017; Hatkevich and Sekelsky 2017; Brady *et al.* 2018; Cox *et al.* 2019; Ruchert *et al.* 2022). Pathogenic variants in *BLM* cause Bloom Syndrome, a rare autosomal recessive disorder characterized by a high predisposition to a broad range of cancers, sun sensitivity, short stature, sterility, and immunodeficiency (Ellis *et al.* 1995; Payne and Hickson 2009; Ababou 2021). *BLM* mutations have also been found in sporadic cancers (Luo *et al.* 2000; Goss *et al.* 2002; Gruber *et al.* 2002; Lindor *et al.* 2017). The high predisposition to cancer in individuals with Bloom Syndrome is associated with genome instability, including high rates of exchange between sister chromatids and homologous chromosomes (Chaganti *et al.* 1974; German *et al.* 1977).

One important function of BLM/Blm in HDR is disassembly of DNA repair intermediates, which is done in concert with topoisomerase III-alpha (TopIIIα) (Karow *et al.* 2000; Van Brabant *et al.* 2000; Wu *et al.* 2000; Bachrati *et al.* 2006). BLM and TopIIIα, together with RMI1 (which *Drosophila* lacks; Sekelsky 2017), unwind D-loops to promote dissociation of the invading strand for synthesis-dependent strand annealing (SDSA) (Van Brabant *et al.* 2000; Adams *et al.* 2003; Cheok *et al.* 2005; Bachrati *et al.* 2006) and catalyze dissolution of double Holliday junctions (dHJs) (Karow *et al.* 2000; Wu and Hickson 2003; Wu *et al.* 2005; Plank *et al.* 2006; Raynard *et al.* 2006). These 2 functions prevent mitotic crossovers and therefore minimize loss of heterozygosity and chromosome rearrangement. Blm orthologs also have functions in meiosis, but these include promoting crossovers (reviewed in Hatkevich and Sekelsky 2017). In *Drosophila*, loss of Blm results in decreased meiotic crossover rates, compromised crossover distribution, and increased chromosome nondisjunction (NDJ) (Hatkevich *et al.* 2017).

BLM/Blm also has functions in repair of stalled replication forks to promote efficient S-phase (Bachrati *et al.* 2006; Wu 2007). BLM accumulates at stalled forks along with other DNA repair regulators, with in vitro studies suggesting BLM may act to regress stalled forks behind a DNA lesion to promote lesion removal by other repair pathways (Ralf *et al.* 2006; Davies *et al.* 2007).

Received on 14 October 2024; accepted on 25 December 2024

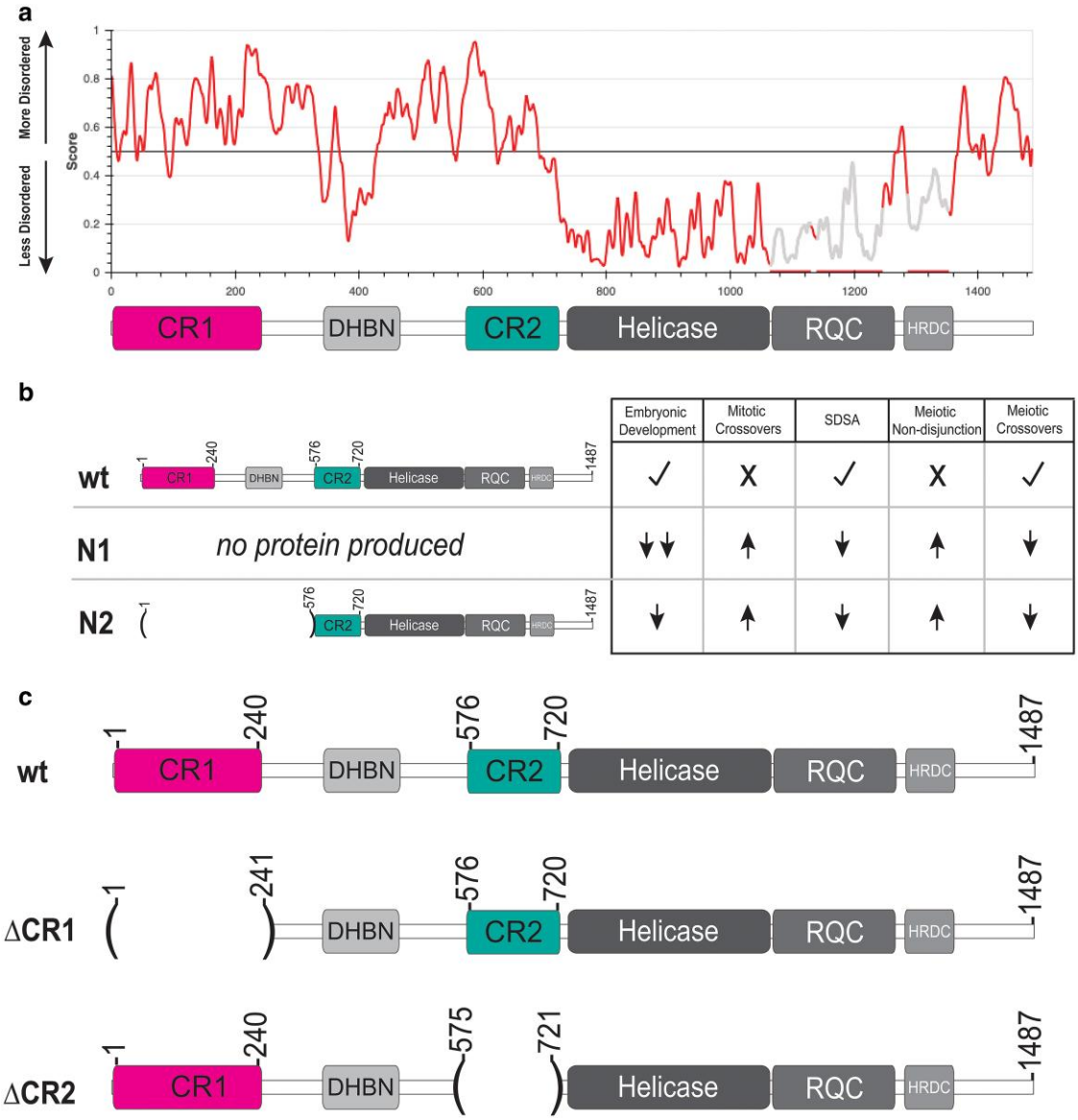

Fig. 1. Blm predicted structural order and alleles used. a) IUPred3 (Cheok *et al.* 2005) plot predicting the ordered and IDRs of Blm. A schematic of Blm domains is placed below for reference, illustrating that conserved regions 1 and 2 (CR1 and CR2) are predicted to be mostly disordered (>0.5). b) Previously characterized alleles of *Blm* and their effects on Blm functions relative to wild-type (wt). A null allele, Blm^{N1} (N1), eliminates all well-characterized Blm functions, while the separation-of-function allele Blm^{N2} (N2) only moderately affects embryonic development. N1 was shown not to produce transcripts, and N2 was shown to produce a protein that lacks the first 575 residues of Blm. c) Schematic of Blm deletions used compared to the wt Blm protein. ΔCR1 deletes amino acids 2–240, preserving residues 241–1487 in frame; ΔCR2 deletes amino acids 576–720, fusing residues 1–575 and 721–1487 in frame.

A second BLM cell cycle role is to resolve anaphase bridges to allow proper chromosome segregation during mitosis (Seki *et al.* 2006; Chan *et al.* 2007). In human cells, this activity is mediated through interaction with topoisomerase IIα (TopIIα) (Russell *et al.* 2011). Micronuclei and aneuploidy are more prevalent in *BLM*-deficient cells, underscoring the importance of this BLM role to genome stability (Mann *et al.* 2005; Naim and Rosselli 2009). In *Drosophila*, embryos lacking Blm have increased anaphase bridges during rapid syncytial cell cycles, resulting in high rates of embryonic death (McVey *et al.* 2007; Ruchert *et al.* 2022). These various functions suggest that BLM/Blm regulation is dependent on cell type and developmental timing.

While BLM/Blm is best known by its RecQ helicase domain, there are intrinsically disordered regions (IDRs) both N- and C-terminal to this domain (Fig. 1a). These regions, though poorly conserved in primary sequence, are likely candidates for both regulatory modifications and protein–protein interactions. TopIIIα is thought to bind in at least one of these regions, and other protein interactions have been mapped to them as well (Wu *et al.* 2000; Russell *et al.* 2011; Grierson *et al.* 2013). Despite this, the IDRs have been relatively poorly explored compared to the helicase domain, even though they make up more than half of the protein (Fig. 1a). A study in *Drosophila* underscores the importance of these regions, with a *Blm* mutation that deletes the first 575 amino acids of the N-terminal IDR (Blm^{N2}) compromising HDR and meiotic roles while only mildly affecting early embryonic functions (Fig. 1b) (McVey *et al.* 2007). This same study also produced alleles that were predicted to delete the first 236 amino acids of Blm (Blm^{N3} and Blm^{N4}), but these were not characterized beyond their mild effects on embryonic development (McVey *et al.* 2007).

To further investigate the function of the N-terminal IDR, we characterized the impacts of deletions of 2 N-terminal regions

conserved in closely related *Drosophila* species on embryonic development, HDR, and meiosis. We find that while deletion of the first 240 amino acids does not compromise Blm functions in meiotic chromosome segregation, it does affect embryonic development, HDR, and meiotic crossover distribution, albeit less severely than *Blm* null mutations. A deletion of the 146 amino acids just prior to the start of the structured RecQ helicase domain results in severe defects in cell division and development but has milder effects on HDR and apparently normal meiotic crossover distribution and segregation. These findings highlight the importance of investigating intrinsically disordered Blm regions to understanding function.

Materials and methods

CRISPR/Cas9 deletion of CR1 and CR2

The endogenous CR1 and CR2 regions of the *Blm* gene (chromosome 3*L*, cytological region 86E17; Öztürk-Çolak *et al.* 2024) were deleted in-frame using CRISPR/Cas9 genome engineering similar to that described in Lamb *et al.* (2017) (Supplementary Fig. 2). A plasmid containing DNA homologous to 5′ and 3′ *Blm* flanking sequence of either CR1 or CR2 (pSL1180 ΔCR1 5′+3′ Homology Arms and pSL1180 ΔCR2 5′+3′ Homology Arms, respectively) and another plasmid containing 5′ and 3′ *Blm* gRNAs for CR1 or CR2 were (pCFD4 *Blm* 1 + 240 gRNA and pCFD4 *Blm* 576 + 720 gRNA, respectively) were simultaneously injected into *Drosophila* embryos expressing Cas9 in their germline stem cells under control of the *nanos* promoter (GenetiVision, Houston, TX). Upon hatching of these embryos, single male progeny were crossed to *TM3,Sb/TM6B, Hu Tb* females to balance potentially edited chromosomes. Once balanced, subsequent single male progeny were again mated to *TM3,Sb/TM6B, Hu Tb* females. After being allowed to mate for 3–4 days at 25 °C, these single males were collected, frozen, and had their genomic DNA isolated to screen for successful deletions by PCR. For vials in which parental males contained the deletion (indicated by a smaller DNA band after PCR compared to wild-type flies), progeny were then mated to siblings to establish a stock. Each deletion stock was then further screened via genomic extraction, PCR, and sequencing of homozygous flies within the resulting stock to confirm the deletion resulted in the correct sequence and that there were no frameshifts. All homozygotes sequenced from each resulting stock contained the correct deletion, flanking sequence, and were not frameshifted, indicating that CR1 and CR2 were successfully deleted.

Embryonic hatching assay

Twenty to thirty virgin females homozygous for each *Blm* allele were crossed to 15 *Oregon-RM* (wild-type) males and allowed to acclimate to grape juice agar plates with yeast paste for 24–36 h at 25 °C. Plates were then changed and embryos were collected overnight (16 h) at 25 °C. One hundred and fifty to three hundred embryos were then transferred to a gridded grape juice agar plate (10/grid) and scored for hatching after 48 h at 25 °C. Hatch assays were completed in 3 replicates for each allelic condition, with a minimum of 550 total embryos assayed per condition.

Mitotic crossover assay

Crossovers were measured in the male germline using the *net* $dpp^{d\text{-}ho}$ *dpy b pr cn* recessive marker chromosome. Virgin females with *net* $dpp^{d\text{-}ho}$ *dpy b pr cn/SM6a* and wild-type or various *Blm* alleles (Blm^{N2}, $Blm^{\Delta CR1}$, or $Blm^{\Delta CR2}$) balanced over *TM6B, Hu Tb* were crossed to *w*; Blm^{N1}/*TM3, Sb* to generate single males heteroallelic (e.g. Blm^{N2}/Blm^{N1}) for *Blm* and heterozygous for recessive phenotypic markers for mitotic crossover analysis. For Blm^{N1} only, virgin females were instead crossed to *w*; Blm^{D2}/*TM3, Sb* to increase the number of progeny obtained for scoring. Single males for each genotype were then crossed to homozygous *net* $dpp^{d\text{-}ho}$ *dpy b pr cn* females and scored for mitotic crossovers. Progeny for each single male was scored as a ratio of crossover progeny to total progeny to generate a mitotic crossover rate for each vial. Data for each genotype were pooled from at least 37 vials and 7,091 progeny to determine the mean mitotic crossover rate.

P{w^a} SDSA assay

The P{w^a} assay was performed as described previously (Adams *et al.* 2003), with minor modifications. First, y^2 w^{Δ} P{w^a} virgin females with wild-type or various *Blm* alleles (Blm^{N1}, Blm^{N2}, $Blm^{\Delta CR1}$, or $Blm^{\Delta CR2}$) balanced over *TM6B, Hu Tb* were crossed to *st* P{*Δ2-3*} Blm^{D2} *Sb/TM6B, Hu Tb* males to generate single males that were heteroallelic for *Blm* (e.g. Blm^{N1}/Blm^{D2}) with the P{w^a} insertion and the Δ2-3 transposase. Blm^{D2} was used because of the availability of a stock with P transposase on the same chromosome. Single males for each genotype were then crossed to y^2 w^{Δ} P{w^a}, and progeny were scored for efficiency of repair by resulting eye color: red indicating efficient SDSA, white/yellow indicating end-joining, and apricot indicating no cutting or perfect repair. Progeny from each single male was scored as a ratio of red-eyed progeny to total progeny as a measure of SDSA repair rate. Data for each genotype were pooled from at least 106 vials and 3,860 progeny to determine the mean SDSA repair rate.

Meiotic NDJ assay

Female meiotic NDJ of the *X* chromosome was measured by first crossing *w*; Blm^{N1}/*TM3, Sb* virgin females to *Oregon-RM* (wild-type) males or males with the *Blm* allele of interest (Blm^{N2}, $Blm^{\Delta CR1}$, or $Blm^{\Delta CR2}$) balanced over either *TM3, Sb* or *TM6B, Hu Tb* to generate heteroallelic *Blm* females (e.g. Blm^{N1}/Blm^{N2}). For experiments with Blm^{N1} only, Blm^{N1} *r e* P{*UASp::Blm*}*/TM6B, Hu Tb* virgin females were crossed to *meiP22*^{103} *st* Blm^{D2} *ry rec*^{1} *Ubx* P{*matα::GAL4*}*/TM6B, Hu Tb* males to generate heteroallelic *Blm* null females that could rescue Blm expression after meiotic recombination to prevent maternal effect lethality in embryos. Heteroallelic *Blm* females were then crossed to *y sc cv v g f/Dp(1;Y)*B^S males. The duplication on the Y chromosome carries a dominant mutation causing bar-shaped eyes. Normal progeny resulting from this cross are females whose eyes are normal and males whose eyes are Bar. Diplo-*X* ova from NDJ give rise to *XXY* females with Bar eyes (and *XXX* embryos that do not survive). Nondisjoined ova that are nullo-*X* result in X0 males (and Y0 progeny who do not survive) whose eyes are *Bar*$^+$. *X* NDJ is calculated as the percentage of progeny that arose from NDJ (*Bar*$^-$ females and *Bar*$^+$ males), correcting for the loss of half of the diplo- and nullo-*X* ova by multiplying this percentage by 2. Crosses were set up as 10 females and 4 males/vial for *Oregon-RM* (wild-type), $Blm^{\Delta CR1}$, and Blm^{N2} genotypes and 30 females and 8 males/vial for $Blm^{\Delta CR2}$ and Blm^{N1} genotypes. Data were pooled from between 15 and 60 vials and at least 1,000 total progeny to determine the mean NDJ rate for each genotype.

Meiotic crossover assay

Meiotic crossovers were measured in the female germline using the *net* $dpp^{d\text{-}ho}$ *dpy b pr cn* recessive phenotypic marker chromosome. Virgin females with *net* $dpp^{d\text{-}ho}$ *dpy b pr cn/SM6a* and wild-type or various *Blm* alleles ($Blm^{\Delta CR1}$ or $Blm^{\Delta CR2}$) combined with *P{matα::GAL4}* for maternal effect lethality rescue were crossed to Blm^{N1} *r e P{UASp::Blm}/TM6B, Hu Tb* to generate females

heteroallelic for *Blm* and heterozygous for recessive phenotypic markers for meiotic crossover analysis. For Blm^{N1} only, *net* $dpp^{d\text{-}ho}$ *dpy b pr cn/CyO;* Blm^{N1} *r e P{UASp::Blm}/TM6B, Hu Tb* virgin females were instead crossed to *mei-*$P22^{103}$ *st* Blm^{D2} *ry* rec^{1} *Ubx P{matα::GAL4}/TM6B, Hu Tb* to rescue the maternal effect lethality in Blm null embryos (Hatkevich *et al.* 2017). Virgin females for each genotype were then crossed to homozygous *net* $dpp^{d\text{-}ho}$ *dpy b pr cn* males and scored for meiotic crossovers indicated by the mixed presence and/or absence of recessive phenotypic markers in progeny. Progeny was scored as a ratio of crossover progeny to total progeny to generate a meiotic crossover rate. Data for each genotype were pooled from at least 15 vials and 3,982 progeny. Crossover density for the entire *net-cn* interval on chromosome 2 (~27 Mb) was calculated using methods described previously (Hatkevich *et al.* 2017).

Structural modeling and analysis of *Drosophila* Blm–TopIIIα interactions

To explore the interactions between the *Drosophila* Blm (UniProt ID: Q9VGI8) and DNA TopIIIα (UniProt ID: Q9NG98), we used AlphaFold v2.3.0 (Jumper *et al.* 2021), a state-of-the-art tool for protein structure prediction. Given the structural relevance and critical interaction interfaces, we selected 2 templates: the DHBN domain of human Blm (PDB ID: 5LUP) (Shi *et al.* 2017) and Blm in complex with DNA (PDB ID: 4CGZ) (Newman and Cooper 2015). Using these templates, we generated 10 models and selected the top-ranked model based on its predicted scores for subsequent analysis. The model's quality was assessed using the predicted TM-score (pTM) and the interchain pTM (ipTM), yielding scores of 0.36 and 0.32, respectively. These scores suggest a moderate confidence level in the overall topology and interchain interactions within the complex. To refine this complex and resolve any steric clashes, we employed the AMBER molecular dynamics suite (Case *et al.* 2023), ensuring the structural stability and accuracy of the model.

We used the PDBsum tool (Laskowski and Thornton 2022) to gain deeper insights into the molecular interactions between Blm–TopIIIα (Supplementary Fig. 3). This tool provided detailed information on the specific residues involved in the Blm–TopIIIα interaction. We used Chimera-X (Pettersen *et al.* 2021) for visualization and rendering high-resolution images to illustrate the molecular interactions within the Blm–TopIIIα complex.

Results

Identification of N-terminal regions conserved among *Drosophila* species and deletion by CRISPR/Cas9 genome editing

Despite high conservation in the helicase domain of Blm, the roughly 720 amino acid N-terminal region is not well conserved among multicellular organisms. This region is predicted to be intrinsically disordered (Fig. 1a). Prior studies, the Blm^{N2} allele, which deletes the first 575 residues of the IDR but retains 146 residues upstream of the helicase domain, pointed to a potential role of this helicase-adjacent N-terminal region in embryonic development (McVey *et al.* 2007). To further examine functions of the N-terminal region, we narrowed our focus to conservation among more closely related *Drosophila* species (Supplementary Fig. 1). Alignment of these species identified 3 regions of high similarity. One of these, from amino acids ~345–460, corresponds to the dimerization helical bundle in N-terminal domain (DHBN) (Shi *et al.* 2017; Hodson *et al.* 2022). We focus here on the other 2 regions, which we term CR1 (Fig. 1c, CR1; residues 1–110) and CR2 (Fig. 1c; CR2; residues 533–720).

We further refined both CR1 and CR2 based on prior data and additional alignment predictions. We expanded CR1 to amino acid 240 to correspond with 1 of the 2 regions in human BLM found to interact with TopIIIα (Wu *et al.* 2000). We also narrowed CR2 to contain only the N-terminal amino acids predicted to be present in the protein produced by the Blm^{N2} allele (amino acids 576–720), to compare their functions more directly. Using CRISPR/Cas9 genome editing, we separately deleted the sequences encoding amino acids 1–240 and 576–720 in the endogenous *Blm* gene (Supplementary Fig. 2). We refer to these alleles as $Blm^{\Delta CR1}$ and $Blm^{\Delta CR2}$ (Fig. 1c).

Embryonic hatch rates are affected differently by each N-terminal Blm deletion

The absence of maternally supplied Blm results in frequent anaphase bridges during syncytial development and high rates of embryonic lethality (McVey *et al.* 2007; Ruchert *et al.* 2022). To determine the effects of each deletion on Blm function in embryonic development, we first conducted embryonic hatching assays. In agreement with prior results, embryos from females homozygous for the Blm^{N1} allele, which does not produce Blm transcript or protein (McVey *et al.* 2007), have severely reduced hatch rates (Fig. 2). In contrast, there is much weaker, though significant, reduction in hatching of embryos from Blm^{N2} mothers. Functionality of the Blm^{N2} protein in embryogenesis likely requires the presence of the helicase, RecQ, and HRDC domains, but the predicted Blm^{N2} protein also has the last 146 residues of the N-terminal IDR that may contribute to function. We assessed the effects of deletion of this region (CR2) on embryogenesis (Fig. 2). Strikingly, embryos from $Blm^{\Delta CR2}$ females have a low hatch rate similar to that of embryos from Blm^{N1} mothers, consistent with this region being critical to Blm function in embryonic development.

The effects of the CR1 deletion are similar to those of Blm^{N2}, with a modest decrease in hatching. While CR1 does have some contribution to embryonic development, both $Blm^{\Delta CR1}$ and Blm^{N2} can be maintained as homozygous stocks.

Mitotic crossovers are moderately elevated in $Blm^{\Delta CR1}$ and $Blm^{\Delta CR2}$ mutants

Flies with the Blm^{N1} or Blm^{N2} deletion have elevated spontaneous mitotic crossovers, probably due at least in part to compromised SDSA and/or dHJ dissolution (Fig. 1b) (McVey *et al.* 2007; Lafave *et al.* 2014). We assayed $Blm^{\Delta CR1}$ and $Blm^{\Delta CR2}$ mutants and found they also have elevated mitotic crossovers (Fig. 3), but at rates (0.27 and 0.51%, respectively) that are significantly lower than those of Blm^{N1} and Blm^{N2} alleles (2.3 and 1.1%, respectively). While Blm^{N2}, $Blm^{\Delta CR1}$, and $Blm^{\Delta CR2}$ were in *trans* to Blm^{N1} in this assay, Blm^{N1} was assayed in *trans* to another allele, Blm^{D2}, a nonsense mutation that gives phenotypes identical to those of Blm^{N1} (McVey *et al.* 2007). Our results suggest that loss of CR1 or CR2 allows some noncrossover repair or some other function that prevents lesions that can be repaired as crossovers.

CR1 and CR2 are required for repair of DSBs by SDSA

Blm has an important role in SDSA, where it is thought to promote dissociation of D-loops during or after repair synthesis (Adams *et al.* 2003; McVey *et al.* 2004). To determine whether the lower number of mitotic crossovers in the $Blm^{\Delta CR1}$ and $Blm^{\Delta CR2}$ mutants relative to null mutants is due to better capabilities of these alleles

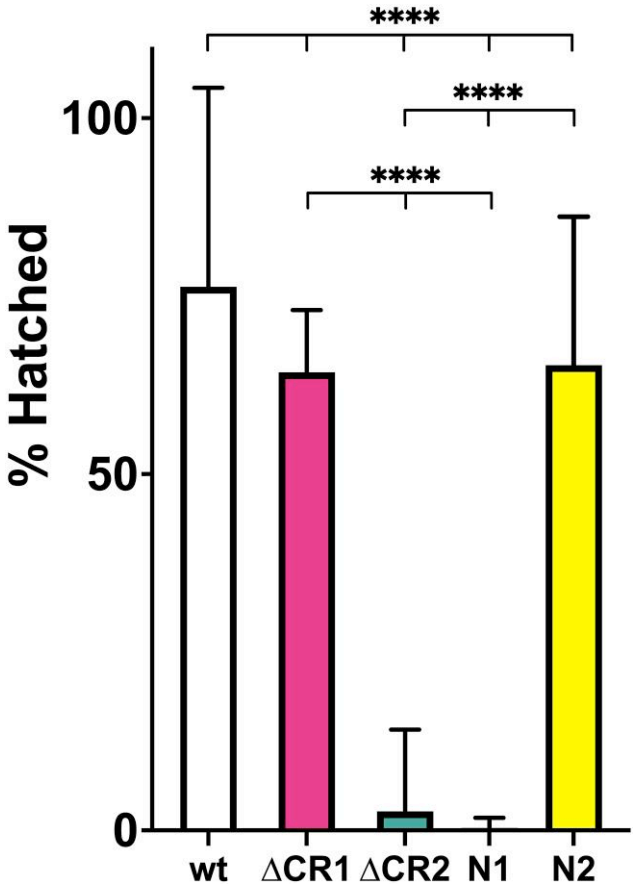

Fig. 2. Hatching of embryos from *Blm* mutant mothers. Virgin females homozygous for the *Blm* alleles indicated on the *X*-axis were crossed to Oregon-RM males and allowed to lay overnight on grape juice agar. Embryos were transferred to fresh grape juice agar plates and scored for hatching 48 h later. Each experiment was repeated 3 times, with 100–250 embryos transferred each time. Significance was determined between each allele by Fisher's exact test. Embryos from $Blm^{\Delta CR2}$ (ΔCR2) or Blm^{N1} (N1) females are rarely able to complete development and are significantly lower in hatch rate compared to wild-type (wt; ****$P < 0.0001$), but not each other ($P = 0.2890$). Embryos from $Blm^{\Delta CR1}$ (ΔCR1) and Blm^{N2} (N2) have a modest but significant reduction in hatch rates compared to wt, but not each other ($P = 0.3334$). All alleles tested had significantly reduced hatch rates compared to wt. We conclude that the CR2 region is more critical for embryonic development but the CR1 region contributes only to a small degree. *n* = wt: 598; ΔCR1: 1,080; ΔCR2: 743; N1: 706; N2: 700. Hatching data are in Supplementary Table 1.

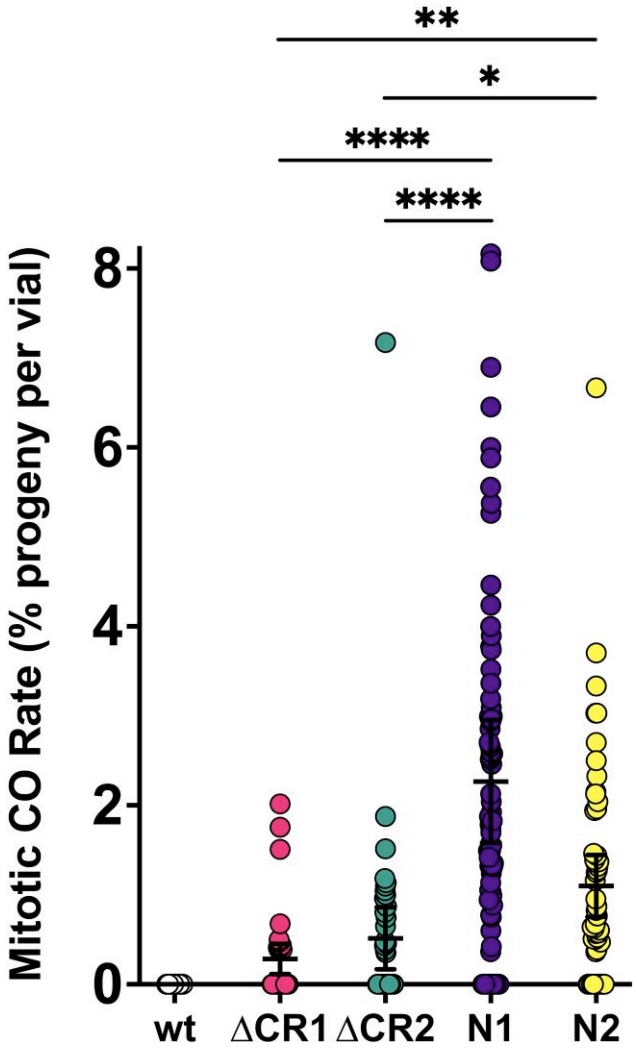

Fig. 3. Mitotic crossovers in *Blm* mutants. We generated males heterozygous for *net* $dpp^{d\text{-}ho}$ *dpy b pr cn* on chromosome 2 and heteroallelic for the *Blm* allele indicated and the amorphic allele Blm^{N1} (Blm^{N1} was assayed in trans to the Blm^{D2} null allele to avoid making any unknown lesions on the Blm^{N1} chromosome homozygous). Single males were crossed to homozygous *net* $dpp^{d\text{-}ho}$ *dpy b pr cn* virgin females, and progeny were scored to detect mitotic crossovers that occurred in the father's germline. Each dot is a biological replicate showing the percentage of progeny arising from a mitotic crossover in 1 vial. Bars show means and standard deviation. Crossovers are extremely rare in wild-type (wt) males (McVey *et al.* 2007), so these were excluded from statistical analyses. While both $Blm^{\Delta CR1}$ (ΔCR1) and $Blm^{\Delta CR2}$ (ΔCR2) have mitotic crossovers, the rates in both mutants are significantly less than that of the Blm^{N1} null mutants (N1). ****$P < 0.0001$ by Kruskal–Wallis with Dunn's multiple comparisons test. Compared to Blm^{N2} separation-of-function mutants, both ΔCR1 and ΔCR2 mutants had significantly fewer mitotic crossovers (**$P < 0.01$ and *$P < 0.05$ by Kruskal–Wallis with Dunn's multiple comparisons test). *n* = wt: 37 vials, 7,091 progeny; ΔCR1: 54 vials, 9,284 progeny; ΔCR2: 44 vials, 7,174 progeny; N1: 88 vials, 9,368 progeny; N2: 54 vials, 7,390 progeny. Mitotic crossover data are in Supplementary Table 2.

to complete SDSA, we conducted the $P\{w^a\}$ SDSA assay (Adams *et al.* 2003; McVey *et al.* 2004). In this assay, effectiveness of SDSA in the male germline is determined by scoring progeny for a red eye color that indicates synthesis of >4,000 bp from each end of a gap generated by transposase-mediated excision, followed by dissociation of nascent strands and annealing of an internal repeat (the long terminal repeat of a *copia* retrotransposon). As reported previously (Adams *et al.* 2003; McVey *et al.* 2007), the red-eye outcome is greatly reduced in Blm^{N1} and Blm^{N2} mutants, demonstrating inability to repair through SDSA. A similar reduction of red-eyed progeny was observed in $Blm^{\Delta CR1}$ and $Blm^{\Delta CR2}$ (Fig. 4), revealing a requirement for both CR1 and CR2 in SDSA.

$Blm^{\Delta CR1}$ and $Blm^{\Delta CR2}$ mutants have distinct meiotic phenotypes compared to Blm^{N1} null mutants

Loss of Blm causes meiotic NDJ (Fig. 1b) (McVey *et al.* 2007; Hatkevich *et al.* 2017). To assess this function in our *Blm* deletion alleles, we performed an *X* chromosome NDJ assay. The rates of NDJ in $Blm^{\Delta CR1}$ (0.5%) and $Blm^{\Delta CR2}$ females (1.33%) were not significantly different from that of wild-type females (Fig. 5), indicating that the regions deleted in CR1 and CR2 are dispensable for Blm functions that prevent NDJ. $Blm^{\Delta CR1}$ and $Blm^{\Delta CR2}$ each also had significantly lower NDJ rates than Blm^{N1} and Blm^{N2} females (7.27 and 6.05%, respectively).

Based on the low NDJ observed in $Blm^{\Delta CR1}$ and $Blm^{\Delta CR2}$ mutants, we hypothesized that they would have normal meiotic crossovers. Surprisingly, crossovers were significantly reduced in $Blm^{\Delta CR1}$

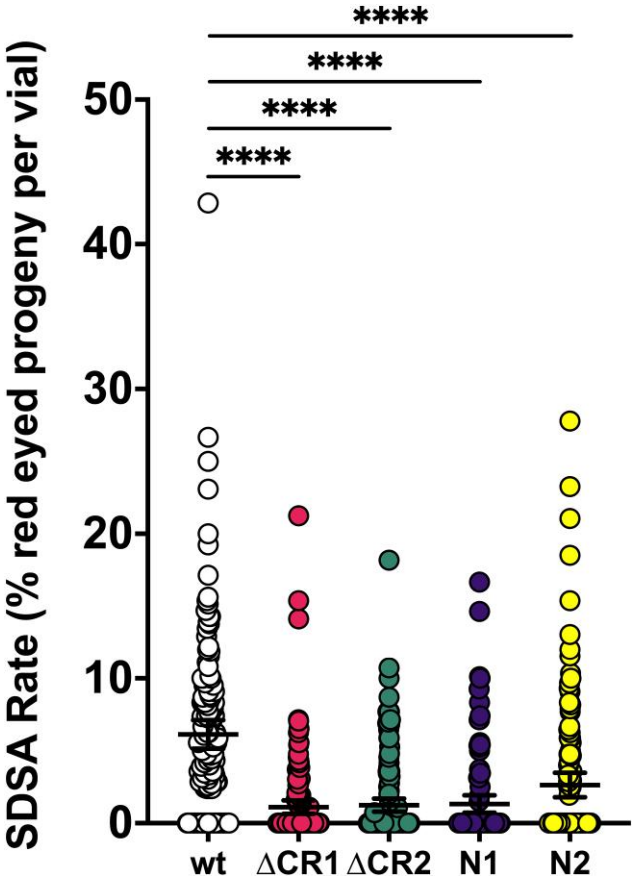

Fig. 4. Repair of DNA gaps by SDSA. Single males with the *Blm* alleles indicated on the X-axis (in *trans* to a Blm^{D2} null allele) and the Δ2-3 transposase were crossed to homozygous $P\{w^a\}$ virgin females, with each vial serving as a biological replicate. Progeny that did not inherit the Δ2-3 transposase were scored for the type of repair that occurred in the parental male's germline, with red eyes indicating completed SDSA, yellow or white eyes indicating end-joining, and apricot eyes indicating either no excision or repair that restored the complete $P\{w^a\}$. SDSA frequency is the percentage of progeny with red eyes. All mutants had significantly lower numbers of red-eyed progeny than wild-type (wt). ****$P < 0.0001$ by ANOVA with Tukey's post hoc and Kruskal–Wallis with Dunn's multiple comparisons. *Blm* mutants were not significantly different from one another ($P > 0.05$ for each comparison). n = wt: 151 vials, 4,675 progeny; ΔCR1: 145 vials, 6,393 progeny; ΔCR2: 148 vials, 4,328 progeny; N1: 106 vials, 4,197 progeny; N2: 133 vials, 3,860 progeny. $P\{w^a\}$ assay dats are in Supplementary Table 3.

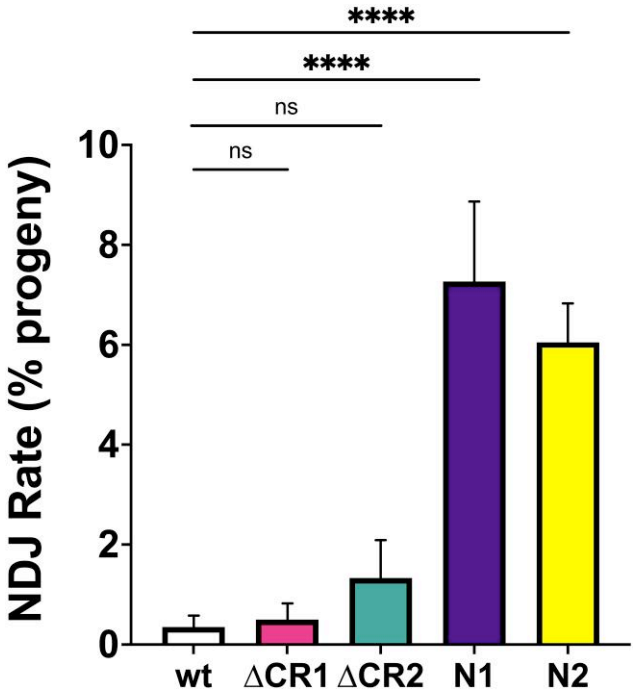

Fig. 5. Meiotic NDJ. Virgin females with the *Blm* alleles indicated on the X-axis over the Blm^{N1} null allele were crossed toy *sc cv v g f/Dp(1;Y)*B^S males in at least 15 vials, each serving as a biological replicate. Progeny were scored for NDJ, indicated by bar eyes in daughters (XXY) and nonbar eyes in sons (X0) genotypes. The number of NDJ progeny was doubled to correct for genotypes that do not progress to adulthood (XXX and Y0), and the NDJ rate was determined as a ratio of the number of corrected NDJ individuals to total progeny for each genotype. Neither $Blm^{\Delta CR1}$ (ΔCR1) nor $Blm^{\Delta CR2}$ (ΔCR2) had a significant increase in NDJ compared to wild-type (wt). In agreement with prior studies, both Blm^{N1} and Blm^{N2} females have significantly elevated NDJ. Blm^{N1} was assayed with an accompanying *P{UASp::Blm}* in *trans* to a chromosome carrying the amorphic allele Blm^{D2} and *P{matα::GAL4}*. The transgenes provide Blm expression after meiotic recombination occurs to provide the essential maternal contribution. This was not necessary for Blm^{N2}. Number of progeny = wt: 6,900; ΔCR1: 3,593; ΔCR2: 1,047; N1: 1,403; N2: 2,975. ****$P < 0.0001$; ns: $P > 0.05$ by the methods described in Zeng *et al.* (2010). NDJ data are in Supplementary Table 4.

mutants (total genetic length of the region assayed was 44.8 cM in $Blm^{\Delta CR1}$ vs 52.4 cM in wild-type, $P < 0.0001$), particularly in the middle of the chromosome arm (Fig. 6). Also surprising was that $Blm^{\Delta CR2}$ mutants had significantly more crossovers (55.3 cM vs 52.4 cM in wild-type females), but with a similar distribution (Fig. 6). These results suggest that CR1 and CR2 have different functions in meiosis, contributing to meiotic crossover distribution in distinct ways.

Structural modeling of CR1, CR2, and the Blm N-terminal IDR

Using the sequences of *Drosophila* Blm and TopIIIα (UniProt IDs: Q9VG18 and Q9NG98), the existing crystal structures of human BLM with DNA (residues 640–1298) plus the dimerization helical in N-terminal (DHBN) domains of human BLM [Protein Data Bank (PDB) codes: 4CGZ and 5LUP, respectively] (Newman and Savitsky 2015; Shi *et al.* 2017), and AlphaFold v2.3.0 (Jumper *et al.* 2021), we were able to generate model to predict structure for the roughly 720 amino acid N-terminal IDR of *Drosophila* Blm bound to *Drosophila* TopIIIα. The top-ranked model revealed 2 Blm-TopIIIα complexes bound to each other along with 2 double-stranded DNA molecules and 2 ADP molecules, providing a detailed view of the protein–protein and protein–DNA interactions (Fig. 7b). While the N-terminal IDR of Blm is predicted to have little structure by itself, this model shows that when in complex with another Blm molecule and 2 accompanying TopIIIα molecules, this region may possess some ordered structure. Notably, our model indicated that both the N-terminal and C-terminal regions of Blm interact with TopIIIα, highlighting key interfaces in the Blm–TopIIIα heterodimeric complex (Fig. 7b; Supplementary Fig. 3). DNA was observed to bind specifically to the winged helix (WH) domain of Blm, where 2 of the strands form a prominent hairpin. This hairpin is suggested to act as a DNA strand separation pin, a function that is consistent with what has been observed in other RecQ helicases (Pike *et al.* 2009; Lucic *et al.* 2011; Kitano *et al.* 2010).

We further sought to focus on the parts of the Blm N-terminal IDR characterized in this work, CR1 and CR2, to better define

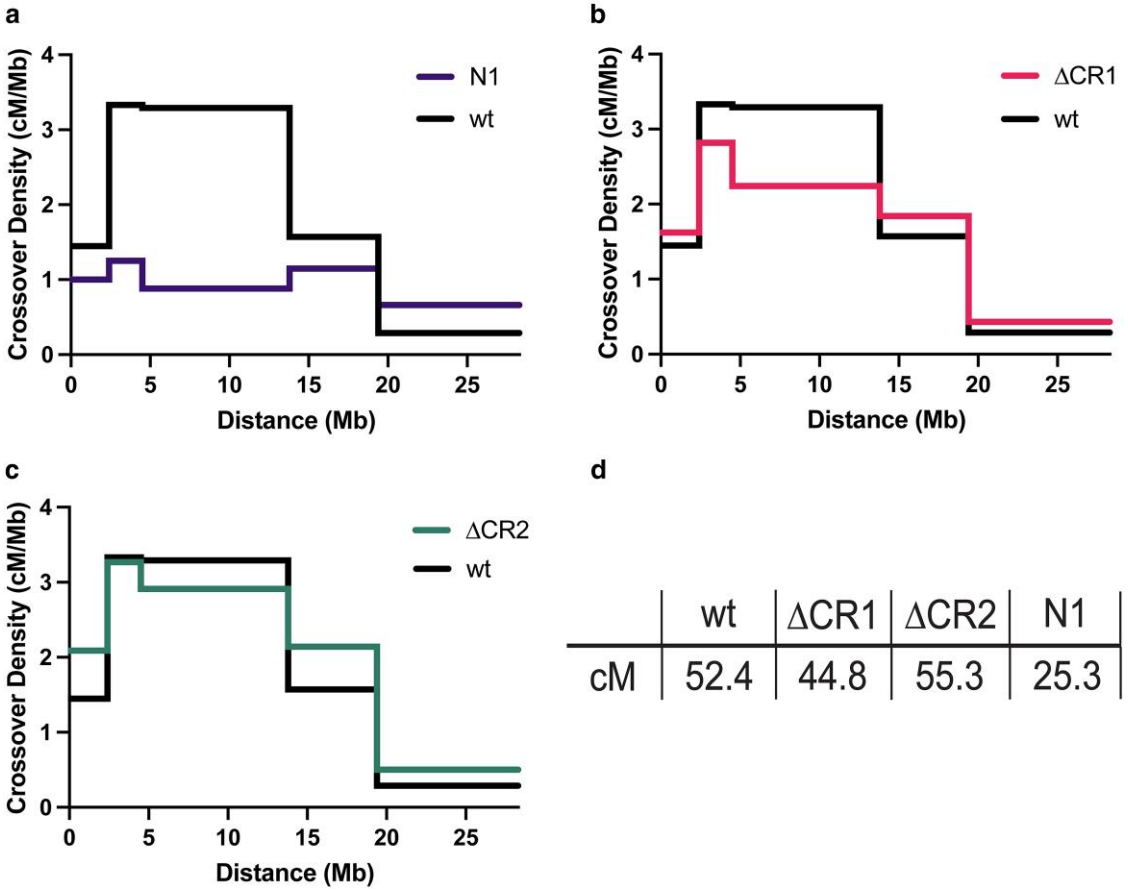

Fig. 6. Meiotic crossovers in *Blm* mutants. Virgin females with the *Blm* alleles indicated on the X-axis (in *trans* to the Blm^{N1} null allele or, in the case Blm^{N1}, to Blm^{D2}) and heterozygous for the *net dpp*^{ho} *dpy b pr cn* chromosome were test crossed, and progeny were scored for recessive phenotypes. Graphs show crossover density (cM/Mb) for each genetic interval. a) Blm^{N1} (N1) had a significant reduction in crossovers and an altered distribution, in agreement with a prior study (Hatkevich *et al.* 2017) ($P < 0.01$ by Fisher's exact test). b) Crossovers were significantly reduced in $Blm^{\Delta CR1}$ (ΔCR1; $P < 0.01$ by Fisher's exact test). c) $Blm^{\Delta CR2}$ (ΔCR2) mutants had a modest but statistically significant increase in crossovers ($P < 0.01$ by Fisher's exact test). d) Both $Blm^{\Delta CR1}$ and $Blm^{\Delta CR2}$ mutants had significantly higher crossing over than Blm^{N1} ($P < 0.0001$ for each, Fisher's exact test for each). $Blm^{\Delta CR1}$ and $Blm^{\Delta CR2}$ mutants were analyzed in the presence of *P{UASp::Blm} P{matα::GAL4}* to rescue any potential maternal effect lethality after meiosis. Blm^{N1} was assayed with an accompanying *P{UASp::Blm}* in *trans* to a Blm^{D2} allele with an accompanying *P{matα::GAL4}* to rescue maternal effect lethality after meiosis to obtain enough progeny for analysis. Comparisons of overall genetic distance (*net* to *cn*) were done between each mutant and wild-type, as described previously (Hatkevich *et al.* 2017). $n = 15$ vials and 4,173 progeny for wt; 77 vials and 3,982 progeny for Blm^{N1}; 107 vials and 4,059 progeny for $Blm^{\Delta CR1}$; 142 vials and 5,087 progeny for $Blm^{\Delta CR2}$. Meiotic crossover data are in Supplementary Table 5.

function. These regions have some predicted contacts with TopIIIα and with the other Blm molecule in the modeled structure. The first 33 residues of CR1 are predicted to interact with TopIIIα, and a significant portion of CR2 (all but the last 20 residues) is predicted to interact (Supplementary Fig. 3). By removing the TopIIIα molecules from the modeled structure, we see that CR1 forms a globular dimer with itself and other slightly downstream regions (Fig. 7c, magenta highlighted region). This may aid the dimerization of DHBN domains of Blm that are slightly C-terminal (approximately amino acids 370–425 in *Drosophila*, amino acids 362–414 in human BLM), supporting a domain shown previously to be critical to Blm self-association (Shi *et al.* 2017; Hodson *et al.* 2022). The CR2 domain, however, is predicted to have very little contacts with the other Blm molecule (Fig. 7c, turquoise highlighted region), suggesting a lesser role than CR1 in supporting Blm dimerization. Based on this model, both regions are likely key to supporting Blm function in distinct ways. CR1 largely appears to have a role in supporting Blm dimerization, but not interaction with TopIIIα, while the opposite is the case for CR2.

Discussion

CR2 is required for embryonic development

We have shown here 2 previously uncharacterized regions of *Drosophila* Blm, CR1 and CR2, have distinct functional roles, summarized in Fig. 7a. Embryos from $Blm^{\Delta CR2}$ homozygous mutant females show compromised hatching, to a similar degree as null mutants. This is likely due to the accumulation of anaphase bridges resulting from defects in rapid replication and/or an inability to resolve sister chromatid entanglements during anaphase. Russell *et al.* (2011) mapped a TopIIα interaction with human BLM to the region that may correspond to CR2 of *Drosophila* Blm. This interaction has not been mapped in *Drosophila* Blm.

It is possible that the CR2 region has regulatory sites to promote or prevent such interaction. Phosphorylation by ataxia-telangiectasia and Rad3^{+} related and mutated (ATR/ATM) kinases might be one way to promote interaction with TopIIα as part of the DNA damage response, both in stalled fork repair and resolution of anaphase bridges. Human ATR phosphorylates BLM at 2 residues to promote the recovery of replication

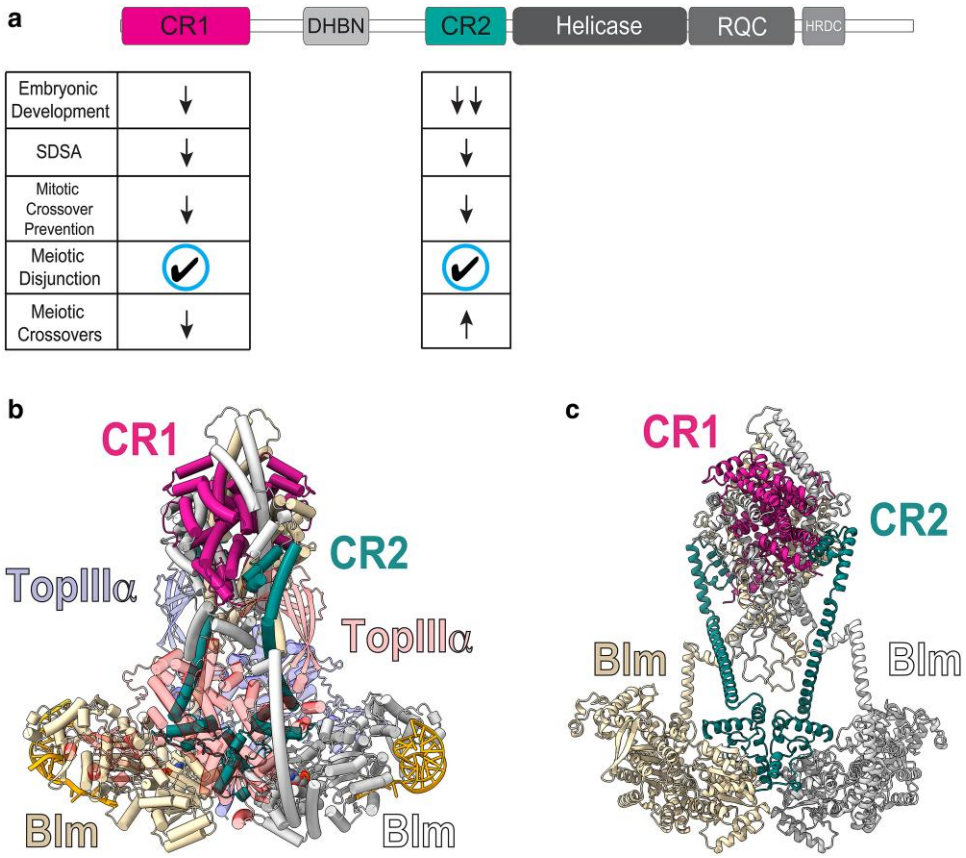

Fig. 7. Summary of CR1 and CR2 effects on Blm functions and model of Blm in complex with TopIIIα. a) Loss of CR1 compromises most Blm functions (down arrows), though not meiotic disjunction (checkmark). Loss of CR2 does not affect meiotic disjunction (checkmark) but does have some effect on SDSA and mitotic crossover prevention (down arrows). Loss of CR2 severely compromises embryonic development (2 down arrows) while slightly increasing meiotic crossovers (up arrow). b) Modeling predicted interaction of Blm and TopIIIα using *Drosophila* Blm and TopIIIα sequences (UniProt IDs: Q9VG18 and Q9NG98) and from existing crystal structures of human BLM with DNA (residues 640–1,298) and the DHBN domains of human BLM (PDB codes 4CGZ and 5LUP, respectively). The 2 molecules of Blm are colored light yellow and white, and the 2 molecules of TopIIIα are light pink and light purple. CR1 is shown in solid magenta and CR2 in solid turquoise for each Blm molecule. While the N-terminus is predicted to be intrinsically disordered in the Blm protein by itself, it appears to have structure when in complex with another Blm protein and 2 TopIIIα proteins. CR2 is predicted to interact extensively with TopIIIα. c) The same structure as in b) with TopIIIα removed and Blm rotated 180° around the Y-axis. CR1 is magenta and CR2 is turquoise. CR1 is predicted to participate in dimerization activity of the N-terminus, while CR2 appears to serve an interaction role.

forks after stalling by hydroxyurea, and mutation of these residues to alanine results in cell cycle arrest (Davies *et al.* 2004). Tangeman *et al.* (2016) found that additional predicted ATR/ATM phosphorylation sites are important for BLM nucleolar localization and TopI interaction. The CR2 region has several S/T-Q sites that are possible targets of ATR/ATM phosphorylation, but a *Drosophila* phosphoproteomic analysis did not identify any phosphopeptides from this region in embryos (Zhai *et al.* 2008).

Harris-Behnfeldt *et al.* (2018) showed a potential requirement for phosphorylation of the human BLM region analogous to *Drosophila* Blm CR2, identifying several residues that when mutated to alanine increase ultrafine anaphase bridges and DNA double-strand breaks while decreasing colocalization of BLM and TopIIα. While some of these residues were predicted to be phosphorylated by ATR/ATM, others were not, suggesting that regulation may be distinct in different species. Regardless of the kinase, regulation and specifically phosphorylation of this region are important to BLM–Blm interaction with TopIIα and function in replication fork repair and resolution of anaphase bridges, even if the residues and kinases involved differ.

CR1 and CR2 are required for SDSA and prevention of mitotic crossovers

Both $Blm^{\Delta CR1}$ and $Blm^{\Delta CR2}$ mutants showed defects in DSB repair (Fig. 7a, SDSA and Mitotic Crossover Prevention boxes). SDSA rates were compromised to the same extent as in Blm^{N1} null mutants, but the frequency of spontaneous mitotic crossovers was not as high as in null mutants. One possibility is that CR1 and CR2 are required for SDSA but not for dHJ dissolution. It is not possible to test this possibility in vivo due to the lack of a dHJ dissolution assay. In addition to conservation, we further chose to study CR1 because it may be analogous to the major TopIIIα-interacting region of human BLM (Wu *et al.* 2000). In vitro, dHJ dissolution requires TopIIIα, which might suggest that $Blm^{\Delta CR1}$ mutants would be defective for dissolution; however, human TopIIIα also interacts with the C-terminus of BLM (Wu *et al.* 2000). Interactions between *Drosophila* Blm and TopIIIα have not been mapped. Furthermore, although BLM can disassemble short D-loops in vitro, it is likely that disassembly of D-loops in vivo, where the ends are not free to rotate, requires topoisomerase activity, so loss of this interaction may impair both SDSA and dHJ dissolution.

How then might each of the Blm deletions studied lead to compromised SDSA? For CR1, it may be that Blm–TopIIIα interaction

with both N- and C-terminal regions of Blm together is necessary for effective SDSA, with loss of either leading to disrupted repair. This could be further explored with a C-terminal deletion in examination of SDSA and mitotic crossovers. Based on the Blm–TopIIIα modeled structure, the CR1–TopIIIα interaction (33 CR1 residues, Fig. 7b; Supplementary Fig. 3) could still be important to full activity Blm in SDSA, with the CR1 also supporting efficient Blm dimerization in this process (Fig. 7c). Future studies could also target ATR/ATM predicted phosphorylation residues within CR1 to attempt to characterize the role of regulation of this region in effective SDSA.

As for the role of CR2 in SDSA, it may be that an interaction with both TopII and TopIIIα is required for this process. While TopIIIα is likely the primary topoisomerase involved in dissolution of D-loops in SDSA, TopII may be necessary to decatenate more complex DNA structures resulting from errors or disrupted repair. The structural model supports extensive interaction with TopIIIα by the CR2 (124 residues, Fig. 7b; Supplementary Fig. 3), and this region may be key to facilitating interactions with other topoisomerases as needed (e.g. TopII), depending on the complexity of the DNA structures present during repair. Future directions will also work to characterize the effects of regulation of CR2 on SDSA, with positive regulation potentially promoting additional interaction and/or stabilization.

CR1 and CR2 contribute to distinct meiotic processes

The 2 deletions caused different meiotic phenotypes (Fig. 7a, Meiotic Disjunction and Meiotic Crossovers boxes). $Blm^{\Delta CR1}$ mutants had a significant reduction in meiotic COs, whereas $Blm^{\Delta CR2}$ mutants had an increase. Neither mutant had increased NDJ. These are both different from *Blm* null mutants, which have decreased meiotic COs, altered CO distribution, and elevated NDJ.

CR1 appears to play a role in meiotic CO distribution, but in a way that is not required for proper segregation of meiotic chromosomes. How loss of this region impacts crossovers but not segregation is unknown. While many of the components involved in meiotic and mitotic DNA repair are conserved, their regulation does often differ in each process. CR1 would be hypothesized to be involved in the resolution of meiotic DSBs as COs, but not in their repair as NCOs. This would be explained by a higher incidence of meiotic NCOs in $Blm^{\Delta CR1}$ mutants. This might be detectable in whole-genome sequencing of progeny to quantify NCOs. Ability of $Blm^{\Delta CR1}$ to resolve any bridged chromosomes during meiotic anaphases could explain the normal NDJ numbers. We should note too that while $Blm^{\Delta CR1}$ CO numbers were significantly lower than wild-type, they were much higher than *Blm* null mutants, so the effects on COs may be mild enough to lead to normal meiotic chromosome segregation.

$Blm^{\Delta CR2}$ meiotic activities are also unusual, with a significant increase of meiotic COs yet normal meiotic disjunction. We speculate that this may be due to an inability of $Blm^{\Delta CR2}$ to resolve DSBs as NCOs, sending more of them into a CO pathway. This would be consistent with CR2, but not CR1, being required for meiotic SDSA and/or dHJ dissolution. In agreement with this hypothesis, overall numbers and patterning of crossovers would not be disrupted, possibly due to $Blm^{\Delta CR2}$ having an intact CR1.

Model of Blm–TopIIIα complex may suggest how CR1 and CR2 function

How does this predicted structure relate to the functions of CR1 and CR2? From the regions of Blm shown in the model to contact TopIIIα, it would seem CR2 is more important than CR1, with a significant portion (124 residues) interacting with the topoisomerase compared to just 33 residues for CR1. From the predicted model and our results from deleting CR2, the CR2–TopIIIα interaction appears to be critical to Blm roles in rapid replication fork progression during embryonic development and SDSA, but less important in preventing mitotic crossovers, meiotic disjunction, and meiotic crossover promotion. One potential explanation for this is that the rapid nature by which replication forks progress in this unique embryonic phase require the CR2–TopIIIα interaction to support the necessary speedy resolution of any stalls, blocks, or damage, which if unrepaired can lead to the characteristic nuclear dropout phenotype seen in Blm mutant embryos (McVey *et al.* 2007; Ruchert *et al.* 2022). This interaction would not be as important at other timepoints and for other Blm–TopIIIα roles. For example, replication fork repair in a typical cell cycle would not be predicted to be affected because checkpoints exist to halt the cell cycle and the cell is not under the pressure to divide rapidly.

While CR1 would appear to be mostly dispensable for interaction of Blm with TopIIIα in this model, its interaction with TopIIIα may still be required in some processes. CR1 is likely somewhat important for homodimerization of Blm, as there are extensive contacts shown between CR1 regions in the Blm homodimer (Fig. 7c), indicating that CR1 may support the DHBN domains' dimerization function. However, given the relatively mild phenotypes for many Blm functions when CR1 is deleted, this dimerization role is probably secondary to the DHBN domains, which are likely the main facilitator of dimerization.

Differences in ΔCR1 and N2 results provide insights into DHBN function

While $Blm^{\Delta CR1}$ and Blm^{N2} mutants have very similar phenotypes in most of the assays reported here, these alleles differ substantially in their effects on meiotic NDJ. A key difference between these alleles is the presence (in $Blm^{\Delta CR1}$) or absence (in Blm^{N2}) of the predicted DHBN domain, suggesting the DHBN contributes to appropriate meiotic chromosome segregation in *Drosophila*. This NDJ may result from a loss of proper meiotic crossover distribution. While this study did not perform a meiotic crossover assay with Blm^{N2}, McVey *et al.* (2007) showed a significant decrease (46%) in meiotic crossovers relative to wild-type over the same net-cn interval used in this study, additionally indicating the DHBN may also be important to meiotic crossover patterning and distribution. These results would also suggest that the meiotic crossover patterning defect is much more severe in Blm^{N2} (46% decrease vs wild-type, McVey *et al.* 2007) compared to $Blm^{\Delta CR1}$ (15% decrease vs wild-type, this study). Deletion of the DHBN may allow confirmation of these roles.

Conclusion

We have assessed genetic functions of N-terminal, unstructured regions of *Drosophila* Blm helicase. We show that deletion of the first 240 amino acids (CR1) does not impair embryonic development or meiotic chromosome segregation but disrupts mitotic DNA repair and meiotic crossover distribution. Deletion of the 146 amino acids upstream of the helicase domain (CR2) leads to severely disrupted embryonic development and aberrant mitotic DNA repair but allows normal meiotic crossover distribution and chromosome segregation. Through this characterization, we have begun to assign distinct Blm functions to different regions of the N-terminus, leading to a better understanding of how this complex protein works to promote development, meiosis, and genome stability.

Data availability

Drosophila stocks are available upon request. The authors confirm that all data necessary for confirming the conclusions of the article are present within the article, figures, table, and supplemental information.

Supplemental material available at GENETICS online.

Acknowledgments

Drosophila stocks obtained from the Bloomington Drosophila Stock Center at the University of Indiana, USA (NIH P40OD018537), were used in this study. We thank members of the Sekelsky lab for helpful comments on the manuscript.

Funding

This work was supported by a grant from the National Institute of General Medical Sciences to JS under award 1R35GM118127. EBD was supported in part by a grant from the National Cancer Institute under award T32CA217824. VRC is supported by the UNC Lineberger Comprehensive Cancer Center Core grant from the National Cancer Institute under award P30CA016086. The funders did not play any role in study design, data collection and analysis, decision to publish, or preparation of the manuscript.

Conflicts of interest

The authors declare no conflicts of interest.

Literature cited

Ababou M. 2021. Bloom syndrome and the underlying causes of genetic instability. Mol Genet Metab. 133(1):35–48. doi:10.1016/j.ymgme.2021.03.003.

Adams MD, McVey M, Sekelsky J. 2003. *Drosophila* BLM in double-strand break repair by synthesis-dependent strand annealing. Science. 299(5604):265–267. doi:10.1126/science.1077198.

Bachrati CZ, Borts RH, ID H. 2006. Mobile D-loops are a preferred substrate for the Bloom's syndrome helicase. Nucleic Acids Res. 34(8):2269–2279. doi:10.1093/nar/gkl258.

Behnfeldt JH, Acharya S, Tangeman L, Gocha AS, Keirsey J, Groden J. 2018. A tri-serine cluster within the topoisomerase IIalpha-interaction domain of the BLM helicase is required for regulating chromosome breakage in human cells. Hum Mol Genet. 27(7):1241–1251. doi:10.1093/hmg/ddy038.

Brady MM, McMahan S, Sekelsky J. 2018. Loss of *Drosophila* Mei-41/ATR alters meiotic crossover patterning. Genetics. 208(2):579–588. doi:10.1534/genetics.117.300634.

Case DA, Aktulga HM, Belfon K, Cerutti DS, Cisneros GA, Cruzeiro VWD, Forouzesh N, Giese TJ, Gotz AW, Gohlke H, *et al.* 2023. AmberTools. J Chem Inf Model. 63(20):6183–6191. doi:10.1021/acs.jcim.3c01153.

Chaganti RS, Schonberg S, German J. 1974. A manyfold increase in sister chromatid exchanges in Bloom's syndrome lymphocytes. Proc Natl Acad Sci USA. 71(11):4508–4512. doi:10.1073/pnas.71.11.4508.

Chan KL, North PS, Hickson ID. 2007. BLM is required for faithful chromosome segregation and its localization defines a class of ultrafine anaphase bridges. EMBO J. 26(14):3397–3409. doi:10.1038/sj.emboj.7601777.

Cheok CF, Wu L, Garcia PL, Janscak P, Hickson ID. 2005. The Bloom's syndrome helicase promotes the annealing of complementary single-stranded DNA. Nucleic Acids Res. 33(12):3932–3941. doi:10.1093/nar/gki712.

Cox RL, Hofley CM, Tatapudy P, Patel RK, Dayani Y, Betcher M, Larocque JR. 2019. Functional conservation of RecQ helicase BLM between humans and *Drosophila melanogaster*. Sci Rep. 9(1):17527. doi:10.1038/s41598-019-54101-5.

Davies SL, North PS, Dart A, Lakin ND, Hickson ID. 2004. Phosphorylation of the Bloom's syndrome helicase and its role in recovery from S-phase arrest. Mol Cell Biol. 24(3):1279–1291. doi:10.1128/MCB.24.3.1279-1291.2004.

Davies SL, North PS, Hickson ID. 2007. Role for BLM in replication-fork restart and suppression of origin firing after replicative stress. Nat Struct Mol Biol. 14(7):677–679. doi:10.1038/nsmb1267.

Dutertre S, Ababou M, Onclercq R, Delic J, Chatton B, Jaulin C, Amor-Gueret M. 2000. Cell cycle regulation of the endogenous wild type Bloom's syndrome DNA helicase. Oncogene. 19(23):2731–2738. doi:10.1038/sj.onc.1203595.

Ellis NA, Groden J, Ye TZ, Straughen J, Lennon DJ, Ciocci S, Proytcheva M, German J. 1995. The Bloom's syndrome gene product is homologous to RecQ helicases. Cell. 83(4):655–666. doi:10.1016/0092-8674(95)90105-1.

German J, Schonberg S, Louie E, Chaganti RS. 1977. Bloom's syndrome. IV. Sister-chromatid exchanges in lymphocytes. Am J Hum Genet. 29:248–255.

Goss KH, Risinger MA, Kordich JJ, Sanz MM, Straughen JE, Slovek LE, Capobianco AJ, German J, Boivin GP, Groden J. 2002. Enhanced tumor formation in mice heterozygous for *Blm* mutation. Science. 297(5589):2051–2053. doi:10.1126/science.1074340.

Grierson PM, Acharya S, Groden J. 2013. Collaborating functions of BLM and DNA topoisomerase I in regulating human rDNA transcription. Mutat Res. 743–744:89–96. doi:10.1016/j.mrfmmm.2012.12.002.

Gruber SB, Ellis NA, Scott KK, Almog R, Kolachana P, Bonner JD, Kirchhoff T, Tomsho LP, Nafa K, Pierce H, *et al.* 2002. BLM heterozygosity and the risk of colorectal cancer. Science. 297(5589):2013. doi:10.1126/science.1074399.

Hatkevich T, Kohl KP, McMahan S, Hartmann MA, Williams AM, Sekelsky J. 2017. Bloom syndrome helicase promotes meiotic crossover patterning and homolog disjunction. Curr Biol. 27(1):96–102. doi:10.1016/j.cub.2016.10.055.

Hatkevich T, Sekelsky J. 2017. Bloom syndrome helicase in meiosis: pro-crossover functions of an anti-crossover protein. Bioessays. 39(9). doi:10.1002/bies.201700073.

Hodson C, Low JKK, Van Twest S, Jones SE, Swuec P, Murphy V, Tsukada K, Fawkes M, Bythell-Douglas R, Davies A, *et al.* 2022. Mechanism of Bloom syndrome complex assembly required for double Holliday junction dissolution and genome stability. Proc Natl Acad Sci USA. 119(6):e2109093119. doi:10.1073/pnas.2109093119.

Imamura O, Fujita K, Shimamoto A, Tanabe H, Takeda S, Furuichi Y, Matsumoto T. 2001. Bloom helicase is involved in DNA surveillance in early S phase in vertebrate cells. Oncogene. 20(10):1143–1151. doi:10.1038/sj.onc.1204195.

Jumper J, Evans R, Pritzel A, Green T, Figurnov M, Ronneberger O, Tunyasuvunakool K, Bates R, Zidek A, Potapenko A, *et al.* 2021. Highly accurate protein structure prediction with AlphaFold. Nature. 596(7873):583–589. doi:10.1038/s41586-021-03819-2.

Karow JK, Constantinou A, Li JL, West SC, ID H. 2000. The Bloom's syndrome gene product promotes branch migration of Holliday junctions. Proc Natl Acad Sci USA. 97(12):6504–6508. doi:10.1073/pnas.100448097.

Kitano K, Kim S-Y, Hakoshima T. 2010. Structural basis for DNA strand separation by the unconventional winged-helix domain of RecQ helicase WRN. Structure. 18(2):177–187. doi:10.1016/j.str.2009.12.011.

Lafave MC, Andersen SL, Stoffregen EP, Holsclaw JK, Kohl KP, Overton LJ, Sekelsky J. 2014. Sources and structures of mitotic crossovers that arise when BLM helicase is absent in *Drosophila*. Genetics. 196(1):107–118. doi:10.1534/genetics.113.158618.

Lamb AM, Walker EA, Wittkopp PJ. 2017. Tools and strategies for scarless allele replacement in *Drosophila* using CRISPR/Cas9. Fly (Austin). 11(1):53–64. doi:10.1080/19336934.2016.1220463.

Larsen NB, Hickson ID. 2013. Recq helicases: conserved guardians of genomic integrity. Adv Exp Med Biol. 767:161–184. doi:10.1007/978-1-4614-5037-5_8.

Laskowski RA, Thornton JM. 2022. PDBsum extras: SARS-CoV-2 and AlphaFold models. Protein Sci. 31(1):283–289. doi:10.1002/pro.4238.

Lindor NM, Larson MC, Derycke MS, Mcdonnell SK, Baheti S, Fogarty ZC, Win AK, Potter JD, Buchanan DD, Clendenning M, *et al.* 2017. Germline miRNA DNA variants and the risk of colorectal cancer by subtype. Genes Chromosomes Cancer. 56(3):177–184. doi:10.1002/gcc.22420.

Lucic B., Zhang Y, King O, Mendoza-Maldonado R, Berti M, Niesen FH, Burgess-Brown NA, Pike ACW, Cooper CDO, Gileadi O, *et al.* 2011. A prominent-hairpin structure in the winged-helix domain of RECQ1 is required for DNA unwinding and oligomer formation. Nucleic Acids Res. 39(5):1703–1717. doi:10.1093/nar/gkq1031.

Luo G, Santoro IM, Mcdaniel LD, Nishijima I, Mills M, Youssoufian H, Vogel H, Schultz RA, Bradley A. 2000. Cancer predisposition caused by elevated mitotic recombination in Bloom mice. Nat Genet. 26(4):424–429. doi:10.1038/82548.

Mann MB, Hodges CA, Barnes E, Vogel H, Hassold TJ, Luo G. 2005. Defective sister-chromatid cohesion, aneuploidy and cancer predisposition in a mouse model of type II Rothmund-Thomson syndrome. Hum Mol Genet. 14(6):813–825. doi:10.1093/hmg/ddi075.

McVey M, Andersen SL, Broze Y, Sekelsky J. 2007. Multiple functions of Drosophila BLM helicase in maintenance of genome stability. Genetics. 176(4):1979–1992. doi:10.1534/genetics.106.070052.

McVey M, Larocque JR, Adams MD, Sekelsky JJ. 2004. Formation of deletions during double-strand break repair in *Drosophila* DmBlm mutants occurs after strand invasion. Proc Natl Acad Sci USA. 101(44):15694–15699. doi:10.1073/pnas.0406157101.

Naim V, Rosselli F. 2009. The FANC pathway and BLM collaborate during mitosis to prevent micro-nucleation and chromosome abnormalities. Nat Cell Biol. 11(6):761–768. doi:10.1038/ncb1883.

Newman JA, Cooper CD, Aitkenhead H, Gileadi O. 2015. Structure of the helicase domain of DNA polymerase theta reveals a possible role in the microhomology-mediated end-joining pathway. Structure. 23(12):2319–2330. doi:10.1016/j.str.2015.10.014.

Newman JA, Savitsky P, Allerston CK, Bizard AH, Ozer O, Sarlos K, Liu Y, Pardon E, Steyaert J, Hickson ID, *et al.* 2015. Crystal structure of the Bloom's syndrome helicase indicates a role for the HRDC domain in conformational changes. Nucleic Acids Res. 43(10):5221–5235. doi:10.1093/nar/gkv373.

Öztürk-Çolak A, Marygold SJ, Antonazzo G, Attrill H, Goutte-Gattat D, Jenkins VK, Matthews BB, Millburn G, dos Santos G, Tabone CJ, and FlyBase Constortium. 2024. FlyBase: updates to the *Drosophila* genes and genomes database. Genetics. 227(1):iyad211. doi:10.1093/genetics/iyad211.

Payne M, Hickson ID. 2009. Genomic instability and cancer: lessons from analysis of Bloom's syndrome. Biochem Soc Trans. 37(3):553–559. doi:10.1042/BST0370553.

Pettersen EF, Goddard TD, Huang CC, Meng EC, Couch GS, Croll TI, Morris JH, Ferrin TE. 2021. UCSF ChimeraX: structure visualization for researchers, educators, and developers. Protein Sci. 30(1):70–82. doi:10.1002/pro.3943.

Pike ACW, Shrestha B, Popuri V, Burgess-Brown N, Muzzolini L, Costantini S, Vindigni A, Gileadi O. 2009. Structure of the human RECQ1 helicase reveals a putative strand-separation pin. Proc Natl Acad Sci. 106(4):1039–1044. doi:10.1073/pnas.0806908106.

Plank JL, Wu J, Hsieh TS. 2006. Topoisomerase IIIa and Bloom's helicase can resolve a mobile double Holliday junction substrate through convergent branch migration. Proc Natl Acad Sci USA. 103(30):11118–11123. doi:10.1073/pnas.0604873103.

Ralf C, Hickson ID, Wu L. 2006. The Bloom's syndrome helicase can promote the regression of a model replication fork. J Biol Chem. 281(32):22839–22846. doi:10.1074/jbc.M604268200.

Raynard S, Bussen W, Sung P. 2006. A double Holliday junction dissolvasome comprising BLM, topoisomerase IIIalpha, and BLAP75. J Biol Chem. 281(20):13861–13864. doi:10.1074/jbc.C600051200.

Ruchert JM, Brady MM, McMahan S, Lacey KJ, Latta LC, Sekelsky J, Stoffregen EP. 2022. Blm helicase facilitates rapid replication of repetitive DNA sequences in early Drosophila development. Genetics. 220(1):iyab169. doi:10.1093/genetics/iyab169.

Russell B, Bhattacharyya S, Keirsey J, Sandy A, Grierson P, Perchiniak E, Kavecansky J, Acharya S, Groden J. 2011. Chromosome breakage is regulated by the interaction of the BLM helicase and topoisomerase IIalpha. Cancer Res. 71(2):561–571. doi:10.1158/0008-5472.CAN-10-1727.

Sekelsky J. 2017. DNA repair in *Drosophila*: mutagens, models, and missing genes. Genetics. 205(2):471–490. doi:10.1534/genetics.116.186759.

Seki M, Nakagawa T, Seki T, Kato G, Tada S, Takahashi Y, Yoshimura A, Kobayashi T, Aoki A, Otsuki M, *et al.* 2006. Bloom helicase and DNA topoisomerase IIIalpha are involved in the dissolution of sister chromatids. Mol Cell Biol. 26(16):6299–6307. doi:10.1128/MCB.00702-06.

Shi J, Chen WF, Zhang B, Fan SH, Ai X, Liu NN, Rety S, Xi XG. 2017. A helical bundle in the N-terminal domain of the BLM helicase mediates dimer and potentially hexamer formation. J Biol Chem. 292(14):5909–5920. doi:10.1074/jbc.M116.761510.

Tangeman L, Mcilhatton MA, Grierson P, Groden J, Acharya S. 2016. Regulation of BLM nucleolar localization. Genes (Basel). 7(9):69. doi:10.3390/genes7090069.

Van Brabant AJ, Ye T, Sanz M, German IJ, Ellis NA, Holloman WK. 2000. Binding and melting of D-loops by the Bloom syndrome helicase. Biochemistry. 39(47):14617–14625. doi:10.1021/bi0018640.

Wu L. 2007. Role of the BLM helicase in replication fork management. DNA Repair (Amst). 6(7):936–944. doi:10.1016/j.dnarep.2007.02.007.

Wu L, Chan KL, Ralf C, Bernstein DA, Garcia PL, Bohr VA, Vindigni A, Janscak P, Keck JL, Hickson ID. 2005. The HRDC domain of BLM is required for the dissolution of double Holliday junctions. EMBO J. 24(14):2679–2687. doi:10.1038/sj.emboj.7600740.

Wu L, Davies S, North P, Goulaouic H, Riou J, Turley H, Gatter K, Hickson I. 2000. The Bloom's syndrome gene product interacts with topoisomerase III. J Biol Chem. 275(13):9636–9644. doi:10.1074/jbc.275.13.9636.

Wu L, Hickson ID. 2003. The Bloom's syndrome helicase suppresses crossing over during homologous recombination. Nature. 426(6968):870–874. doi:10.1038/nature02253.

Zeng Y, Li H, Schweppe NM, Hawley RS, Gilliland WD. 2010. Statistical analysis of nondisjunction assays in *Drosophila*. Genetics. 186(2):505–513. doi:10.1534/genetics.110.118778.

Zhai B, Villen J, Beausoleil SA, Mintseris J, Gygi SP. 2008. Phosphoproteome analysis of *Drosophila melanogaster* embryos. J Proteome Res. 7(4):1675–1682. doi:10.1021/pr700696a.

Editor: B. Calvi